Physica B 407 (2012) 3188–3191

Contents lists available at SciVerse ScienceDirect

Physica B

journal homepage: www.elsevier.com/locate/physb

Electronic structure and properties of NbS_2 and TiS_2 low dimensional structures

F. Güller [a,b,*], C. Helman [a], A.M. Llois [a,b,c]

[a] Centro Atómico Constituyentes, GIyANN, CNEA, San Martín, Buenos Aires, Argentina
[b] Consejo Nacional de Investigaciones Científicas y Técnicas, C1033AAJ Buenos Aires, Argentina
[c] Departamento de Física Juan José Giambiagi, FCEyN, UBA, Buenos Aires, Argentina

ARTICLE INFO

Available online 4 January 2012

Keywords:
Dichalcogenides
Graphene like
Low dimension

ABSTRACT

Transition metal dichalcogenides have a laminar structure, weakly bound through van der Waals interactions. Due to their technological applications in catalytic processes the bulk structure of many of them has been widely studied in the last 30 years. Some of them, such as $NbTe_2$ and $TiSe_2$, show superconductivity and have been, therefore, the subject of intense study. Novoselov et al. (2005 [1]) achieved to isolate not only graphene but also other bidimensional crystals, among them layers of some dichalcogenides. These bidimensional crystals preserve their monocrystallinity under normal ambient conditions, keeping the crystal structure of the bulk. In this contribution we calculate the magnetic and electronic properties of 2D layers of NbS_2 (non-magnetic metal in 3D) and TiS_2 (non-magnetic semimetal in 3D) as well as quasi 1D chains cut out from these layers.

1. Introduction

Transition metal dichalcogenides MX_2, where M denotes the transition metal and X stands for S, Se or Te, are well known for their layered quasi 2D structure. Atoms within a layer are bound covalently and separate layers are held together mainly through weak van der Waals interactions. Each layer, actually a trilayer, is composed by a plane of metal atoms situated in between two planes of chalcogen atoms (X–M–X). There exist two stacking possibilities (polytypes) for these layered structures, called 1T and 2H. The 1T and 2H trilayers differ only in the relative position of the two chalcogen planes. In the 1T (2H) structure each metal atom has octahedral (trigonal prismatic) coordination.

The electronic and structural properties of bulk transition metal dichalcogenides (TMDC) have been widely studied for the last three decades due to their many potential technological applications. Some of these compounds exhibit charge density wave phenomena and superconductivity [2–4]. Bulk transition metal disulphides (MS_2), in general, have received special attention due to their uses in the petroleum industry as catalysts and lubricants [5–7].

Recently, Novoselov et al. have successfully isolated single layers of graphene and other laminar compounds, among them some TMDC [1]. This opens the path for investigation of many 2D crystals, as well as 1D structures such as ribbons and nanotubes cut out from these 2D layers. So far most efforts have been concentrated on graphene, which has already revealed remarkable new phenomena (see Ref. [8] and references therein). The same can be said about graphene nanoribbons and carbon nanotubes (see for example Ref. [9]). TDMC, however, have received far less attention.

In this contribution, we report *ab initio* calculations of electronic and magnetic properties of 2D trilayers and zig-zag and armchair 1D chains of TiS_2 and NbS_2. First we explain technicalities about the calculations. Then the main characteristics of the 2D trilayers and the 1D chains are discussed. Finally we present our conclusions.

2. Computational details

Calculations are performed using *ab initio* density functional theory as implemented in the WIEN2k [10] and VASP [11] codes. Structural parameters are optimized using VASP with PAW pseudopotentials [12] considering the smallest possible unit cells. The positions of the ions are relaxed until all forces are smaller than 0.04 eV/Å. The spin polarized electronic properties of the relaxed and unrelaxed structures are obtained using WIEN2k. The values of the muffin-tin radii are set to 1.06 Å and 0.95 Å for metal atoms and S atoms, respectively, and the plane waves cutoff parameter is $R_{mt}*K_{max}=7$. The considered atomic valence configurations are $3s^23p^4$ for S, $3s^23p^63d^24s^2$ for Ti and $4s^24p^64d^45s^1$ for Nb. All the calculations are done using the generalized

* Corresponding author at: Centro Atómico Constituyentes, GIyANN, CNEA, San Martín, Buenos Aires, Argentina.
E-mail address: guller@tandar.cnea.gov.ar (F. Güller).

0921-4526/$ - see front matter © 2012 Elsevier B.V. All rights reserved.
doi:10.1016/j.physb.2011.12.061

gradient approximation as parameterized by Perdew et al. [13] for the exchange and correlation potential.

To model the infinite 2D trilayers, a supercell with 10 Å vacuum between each trilayer is used. For this supercell 867 k-points in the first Brillouin zone are enough to achieve the desired accuracy. The supercell for 1D structures (chains) has 10 Å vacuum in the two perpendicular directions, avoiding chains to interact with each other when the periodic calculations are performed. In that case 220 k-points in the first Brillouin zone prove to be sufficient.

3. Results

3.1. 2D trilayers

Schematic representations of the 2H and 1T trilayers are shown in Fig. 1. Metal atoms are arranged in a hexagonal lattice with constant a. The S atoms are situated at $(1/3\ a, 2/3\ a, \pm t/2)$ for the 2H structure and $\{(2/3\ a, 1/3\ a, -t/2);(1/3\ a, 2/3\ a, t/2)\}$ for the 1T structure. The direction $\hat{z}$ is perpendicular to the layers and the parameter t is the layer thickness. Both a and t depend on the specific compound. Table 1 shows the optimized lattice parameters of the compounds under study and the experimental bulk ones [14,15]. The optimized constants obtained for the TiS_2 trilayer turn out to be practically identical to the experimental bulk values. Those of the NbS_2 layer are approximately 4% larger than the corresponding bulk experimental ones. As expected, the electronic structure of the trilayers is strongly molecular like, with the charge density concentrated along covalent bonds. Fig. 2 shows a side view of the valence charge density of a NbS_2 trilayer. The total spin polarized density of states of the NbS_2 and TiS_2 trilayers are shown in Figs. 3 and 4, respectively. The TiS_2 trilayer is non-magnetic semiconducting with a small gap of approximately 0.1 eV. This semiconducting behaviour is in agreement with other DFT calculations [16,17], although the band gap width is controversial, while experimental results are pending. For the NbS_2 trilayer we obtain metallic behaviour. The DOS exhibits a high peak near the Fermi level. Also, a small magnetic moment of 0.28 μB per Nb atom appears. In both cases contributions to the electronic states come mainly from the S atom p-type orbitals and the metal atom d-type orbitals. The same occurs in the 1D structures, discussed in the following section, and in the bulk compounds (not shown). The character of the electronic states is preserved.

3.2. 1D chains

By slicing the 2D TiS_2 and NbS_2 trilayers one can obtain 1D stripes, or ribbons, as in the better known case of graphene. The 2D layers can be cut in several ways, producing ribbons with different types of edges. As in the case of graphene nanoribbons, the two simplest edge types are the so-called zig-zag and armchair. These edges preserve the stoichiometry of the bulk. The narrowest possible structures of each edge type are shown in Fig. 5. Structurally, the optimized chains are significantly different from the unrelaxed ones (see Fig. 5). The optimized lattice constants of the NbS_2 chains are

Table 1
Optimized parameters of the 2D trilayers and experimental parameters of the bulk compound. a is the hexagonal lattice constant. t is the layer thickness.

Parameter type	NbS_2		TiS_2	
	a (Å)	t (Å)	a (Å)	t (Å)
Theoretical (2D)	3.35	3.11	3.40	2.82
Experimental (bulk)	3.30 [14]	2.97 [14]	3.40 [15]	2.83 [15]

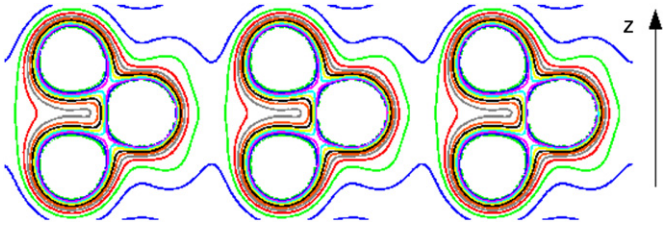

Fig. 2. Valence charge density contours of a NbS_2 trilayer along the bonding plane depicted in Fig. 1c. The $\hat{z}$ direction is perpendicular to the trilayer. The Nb atoms at the centre of the trilayer are bonded covalently to two S atoms lying above and below.

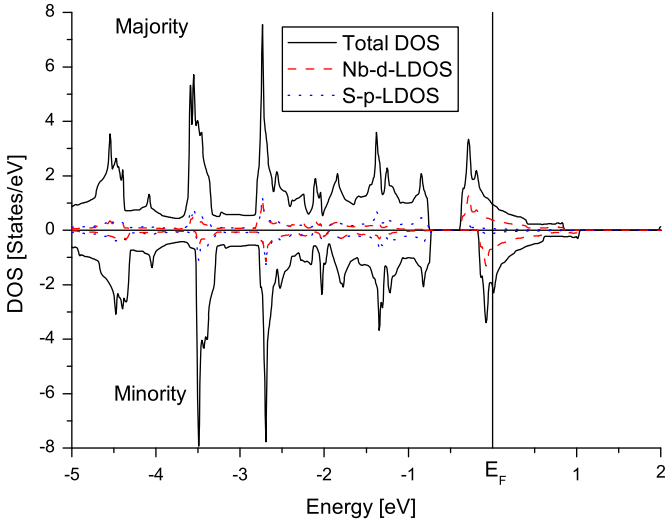

Fig. 3. Spin polarized density of states of 2D-NbS_2. The magnetic moment per Nb atom is 0.28 μB/Nb.

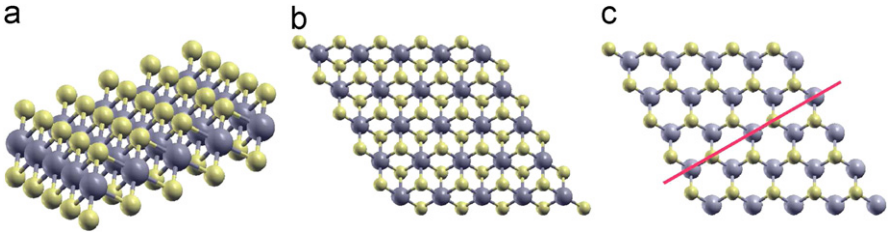

Fig. 1. Possible TMDC 2D trilayer structures. Dark grey atoms are metallic. (a) and (b) are two different views of TiS_2 trilayer (1T polytype). (c) Top view of NbS_2 (2H polytype). The straight line shows the perpendicular bonding plane used in the plot of Fig. 2.

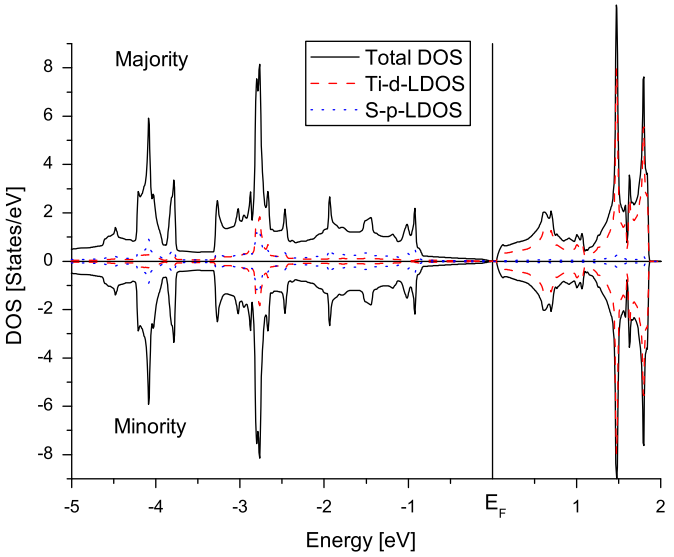

Fig. 4. Spin polarized density of states of 2D-TiS_2. There is a small gap of approximately 0.1 eV between valence and conduction bands.

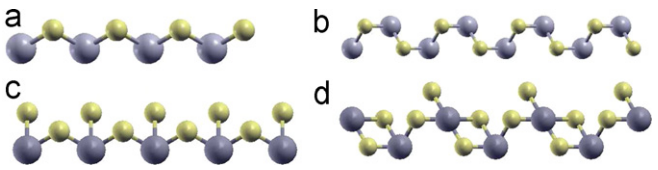

Fig. 5. As cut chains from 2D trilayers. (a) NbS_2 zig-zag. (b) NbS_2 armchair. (c) TiS_2 zig-zag. (d) $TiS2_2$ armchair.

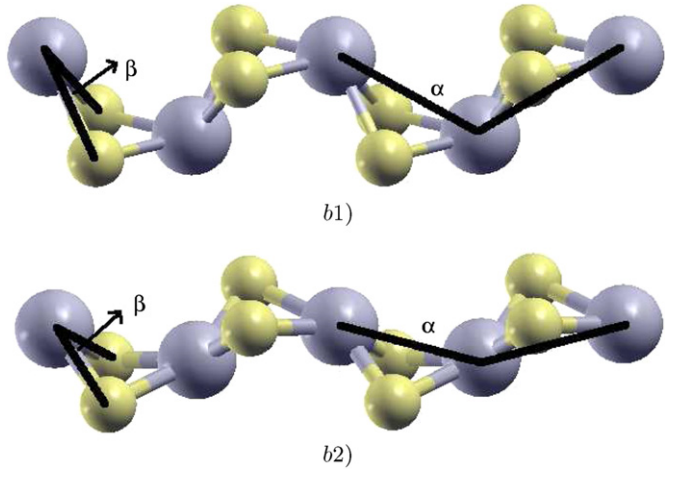

Fig. 6. NbS_2 armchair chains compared before and after atomic relaxation. (b1) As cut (unrelaxed). (b2) Relaxed. Angles α and β change from 120° to 153° and 77° to 42° respectively. The distance between two successive Nb atoms changes from 3.35 Å to 2.97 Å.

approximately 2% smaller than the corresponding 2D ones. The ones of the TiS_2 chains are larger by approximately 15% in the zig-zag case and 2% in the armchair case. As an example, in Fig. 6, we show the as cut and relaxed NbS_2 armchair chains (see Fig. 5b). The spin polarized electronic structure of the as cut and relaxed chains are obtained considering only colinear spin configurations. The lowest energy magnetic configuration of most chains changes upon relaxation. Table 2 shows the energy difference between the ferromagnetic (FM) and antiferromagnetic (AFM) configurations, $\Delta E_{(AFM\text{-}FM)}$, along with the corresponding magnetic moments for the studied chains. The relaxed TiS_2 chains are non-magnetic, while the as cut parent systems are magnetic. In the case of NbS_2 the zig-zag chain presents half metallic character before and after relaxation, indicating the stability of this electronic configuration for this system. The spin polarized density of states of the relaxed chain is shown in Fig. 7. The armchair NbS_2 chain is metallic and slightly AFM after relaxation, but the energy difference between FM and AFM configurations is very small.

4. Conclusions

In this contribution we obtain the electronic properties of 2D trilayers and 1D chains of NbS_2 and TiS_2. Bulk NbS_2 is metallic and this metallic character is preserved when going down in dimensionality to the 2D trilayer and the 1D chains. The bulk system is non-magnetic, but all the low dimensional structures here studied show magnetic order, even if the only relaxed nanostructure with a large energy difference between FM and AFM configurations is the 1D zig-zag chain, which is additionally half metallic.

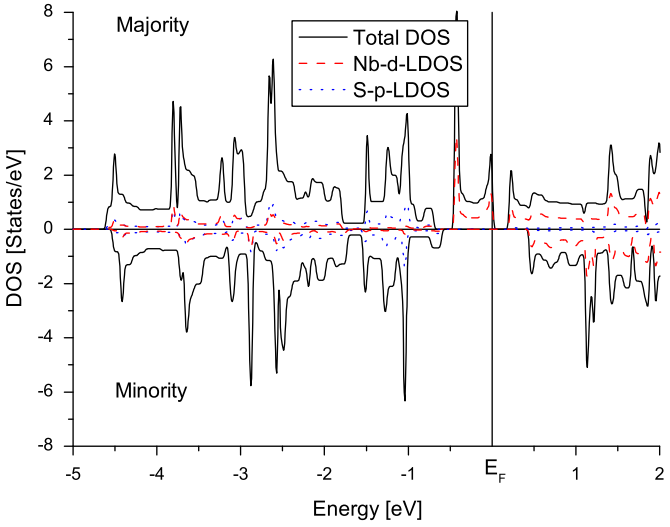

Fig. 7. Spin polarized density of states of the NbS_2 zig-zag relaxed chain. Note the half-metallic character.

Table 2
$\Delta E_{(AFM\text{-}FM)}$ is the energy difference between the antiferromagnetic and ferromagnetic spin configurations per metallic atom for relaxed and unrelaxed chains. The corresponding magnetic moments for the most stable configuration are also shown. Due to the highly asymmetric structure of the as cut TiS_2 chain, all atoms in the cell have different magnetic moments. All Ti atoms have the same polarization while S atoms have the opposite polarization. The values shown are average magnetic moments of each species.

Chain type	NbS_2 zig-zag		TiS_2 zig-zag		NbS_2 armchair		TiS_2 armchair	
	As cut	Relaxed	As cut	Relaxed	As cut	Relaxed	As cut	Relaxed
$\Delta E_{(AFM-FM)}$ (eV)	0.15	0.06	0.04	0	0.06	−0.005	−0.005	0
Magnetic moment and order	$1\mu_B$/Nb (FM)	$1\mu_B$/Nb (FM)	$0.48\mu_B$/Ti (FM)	$0\mu_B$/atom	$1\mu_B$/Nb (FM)	$0.15\mu_B$/Nb (AFM)	$0.18\mu_B$/Ti atom $-0.09\mu_B$/S atom	$0\mu_B$/atom

Bulk TiS_2 is a non-magnetic semimetal. The low dimensional relaxed systems considered are also non-magnetic, but the metallic character disappears in the 2D trilayer.

In future work we will relax the 1D chains considering larger unit cells to allow for eventual dimerization and more flexibility to the systems.

Acknowledgements

The authors acknowledge the financial support from ANPCyT and CONICET (PRH74 and PIP-0258) and UBACyT-X123.

References

[1] K.S. Novoselov, D. Jiang, F. Schnedin, T.J. Booth, V.V. Khotkevitch, S.V. Morozov, A.K. Geim, Proc. Natl. Acad. Sci. USA 120 (2005) 10451.
[2] J.A. Wilson, F.J. DiSalvo, S. Mahajan, Adv. Phys. 24 (1975) 117.
[3] R.H. Friend, D. Jerome, J. Phys. C 12 (1979) 1441.
[4] F.J. DiSalvo, Physica B and C 105 (1981) 3.
[5] T.A. Pecoraro, R.R. Chinanelli, J. Catal. 67 (1981) 430.
[6] P.D. Fleischauer, J.R. Lince, P.A. Bertrand, R. Bauer, Langmuir 5 (1989) 1009.
[7] P. Raybaud, J. Hafner, G. Kresse, H. Toulhoat, J. Phys.: Condens. Matter 9 (1997) 11107.
[8] A.K. Geim, K.S. Novoselov, Nat. Mater. 6 (2007) 183.
[9] A. Jorio, M.S. Dresselhaus, G. Dresselhaus, Carbon nanotubes: advanced topics in the synthesis, structure, properties and applications, Topics in Applied Physics, vol. 111, Springer, 2008.
[10] P. Blaha, K. Schwarz, G.K.H. Madsen, D. Kvasnicka, J. Luitz, WIEN2k, An Augmented Plane Wave+Local Orbitals Program for Calculating Crystal Properties, Technical Universitt, Wien, Austria, 2010.
[11] G. Kresse, J. Fruthmüller, Phys. Rev. B 54 (1996) 11169.
[12] G. Kresse, D. Joubert, Phys. Rev. B 59 (1999) 1758.
[13] J. P Perdew, K. Burke, Y. Wang, Phys. Rev. B 54 (1996) 16533.
[14] F. Jellinek, G. Brauer, H. Müller, Nature 185 (1960) 376.
[15] D.R. Allan, A.A. Kelsey, S.J. Clark, R.J. Angel, G.J. Ackland, Phys. Rev. B 57 (1998) 5106.
[16] V.V. Ivanovskaya, G. Seifert, A.L. Ivanovskii, Semiconductors 39 (2005) 1058.
[17] C.M. Fang, R.A. de Groot, C. Haas, Phys. Rev. B 56 (1997) 4455.